Real-time imaging of electrical signals with an infrared FDA-approved dye

Supporting Information

Jeremy S. Treger,* ¶ Michael F. Priest,† ¶ Raymond Iezzi,‡ and Francisco Bezanilla*†

*Department of Biochemistry and Molecular Biology, University of Chicago, Chicago, IL;
†Committee on Neurobiology, University of Chicago, Chicago, IL;
‡Department of Ophthalmology, Mayo Clinic, Rochester, MN;
¶These authors contributed equally

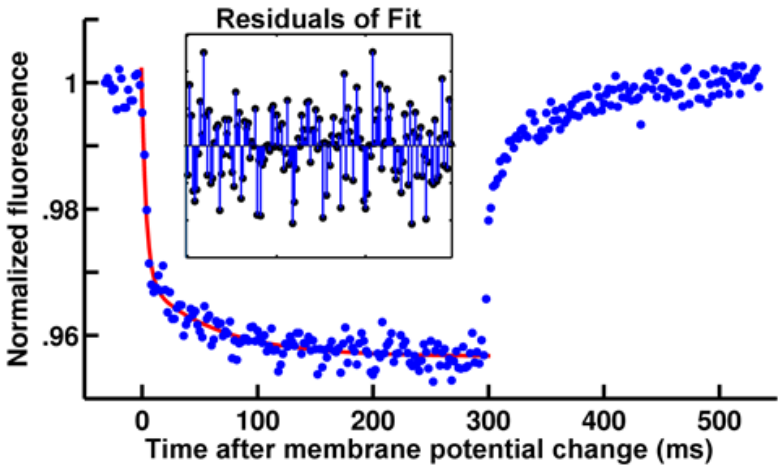

Figure S1: Kinetics of the indocyanine green voltage-sensitive response. The kinetics of the change in fluorescence of ICG in response to a change in membrane potential (*blue*) can be fit by a double exponential function (*red line*, see inset for residuals). The time constant of the faster component, which comprises the majority of the fluorescence change, was 4.0 ms, while the time constant of the slower component was 62 ms. During this recording the time constant of the voltage-clamp was 150 μs; the camera was running at a 500 Hz frame rate.

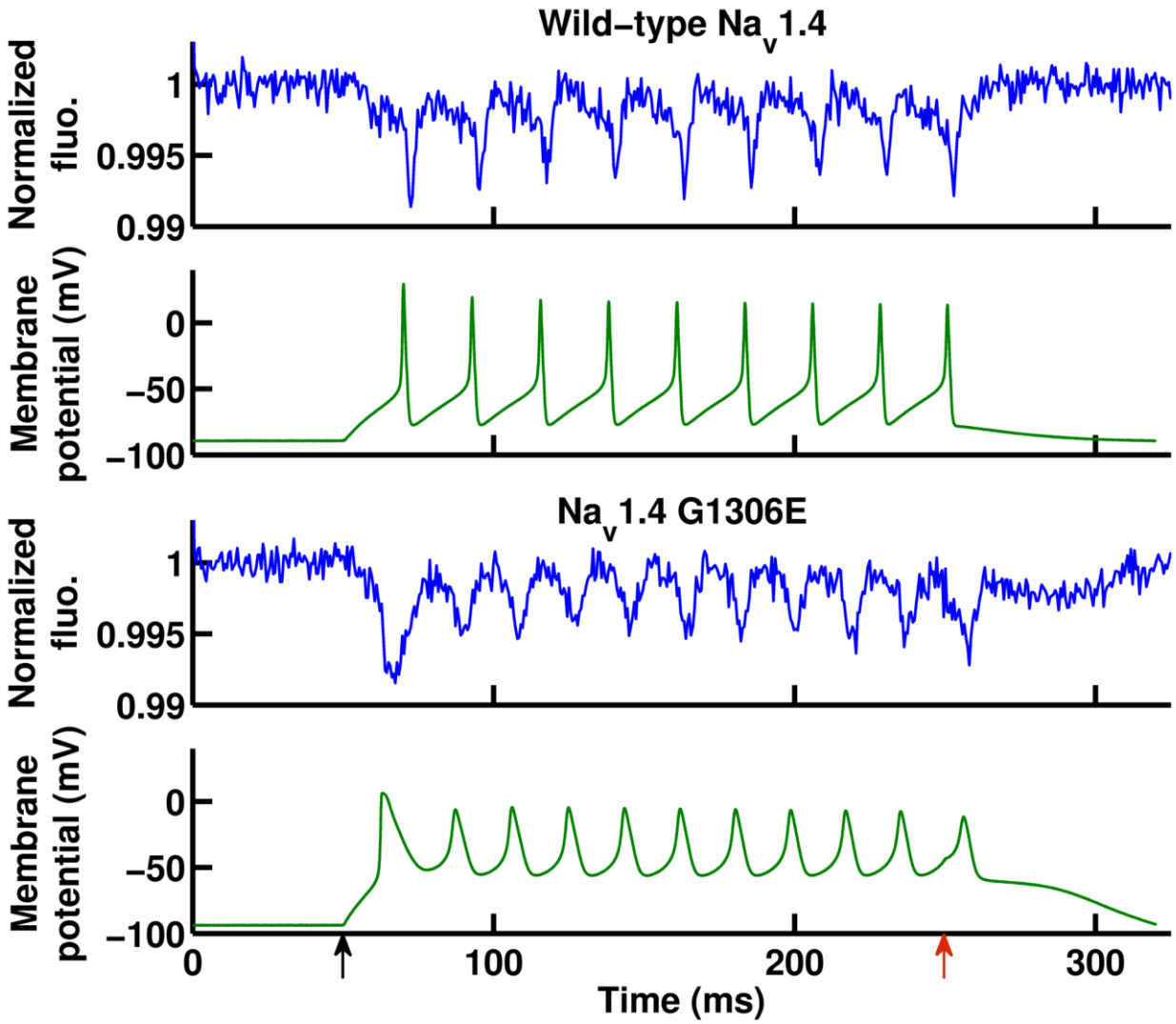

Figure S2: ICG follows the shapes of action potentials. ICG fluorescence (*blue*, upper rows of each construct) follows action potentials (*green*, lower rows) fired by excitocytes in response to an injection of current (beginning at black arrow and ending at red arrow). The fluorescence follows the shape of the action potentials, discriminating between action potentials generated by wild-type $Na_v1.4$ (top pair, full time course of Fig. 2 *B*) and action potentials generated by mutant $Na_v1.4$ with the G1306E myotonia substitution (bottom pair, full time course of Fig. 2 *C*).

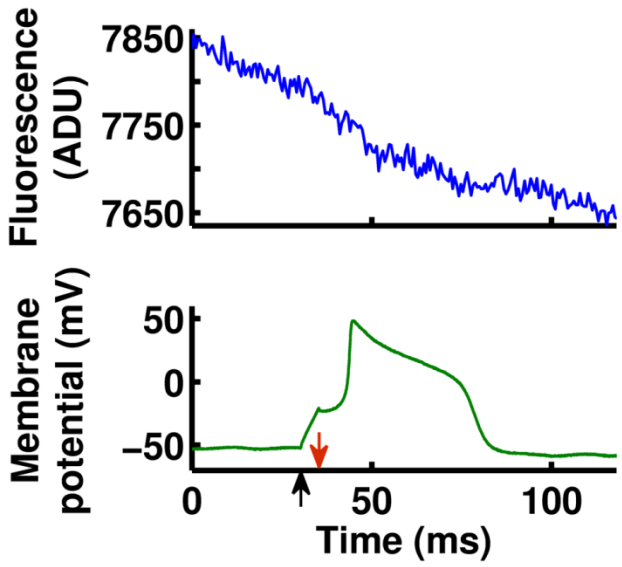

Figure S3: Unprocessed data from cultured rat neurons demonstrates voltage sensitivity. Unprocessed data of ICG fluorescence from Fig. 3 *A* in the main text (*top, blue*). This is an average of all pixels in the field of view, including those outside of the neuron, causing the reduction in signal to noise. Additionally, no bleach correction or filtering has been applied. An injection of depolarizing current was given from the black arrow until the red arrow, resulting in an action potential (*bottom, green*, identical to Fig. 3 *A*).

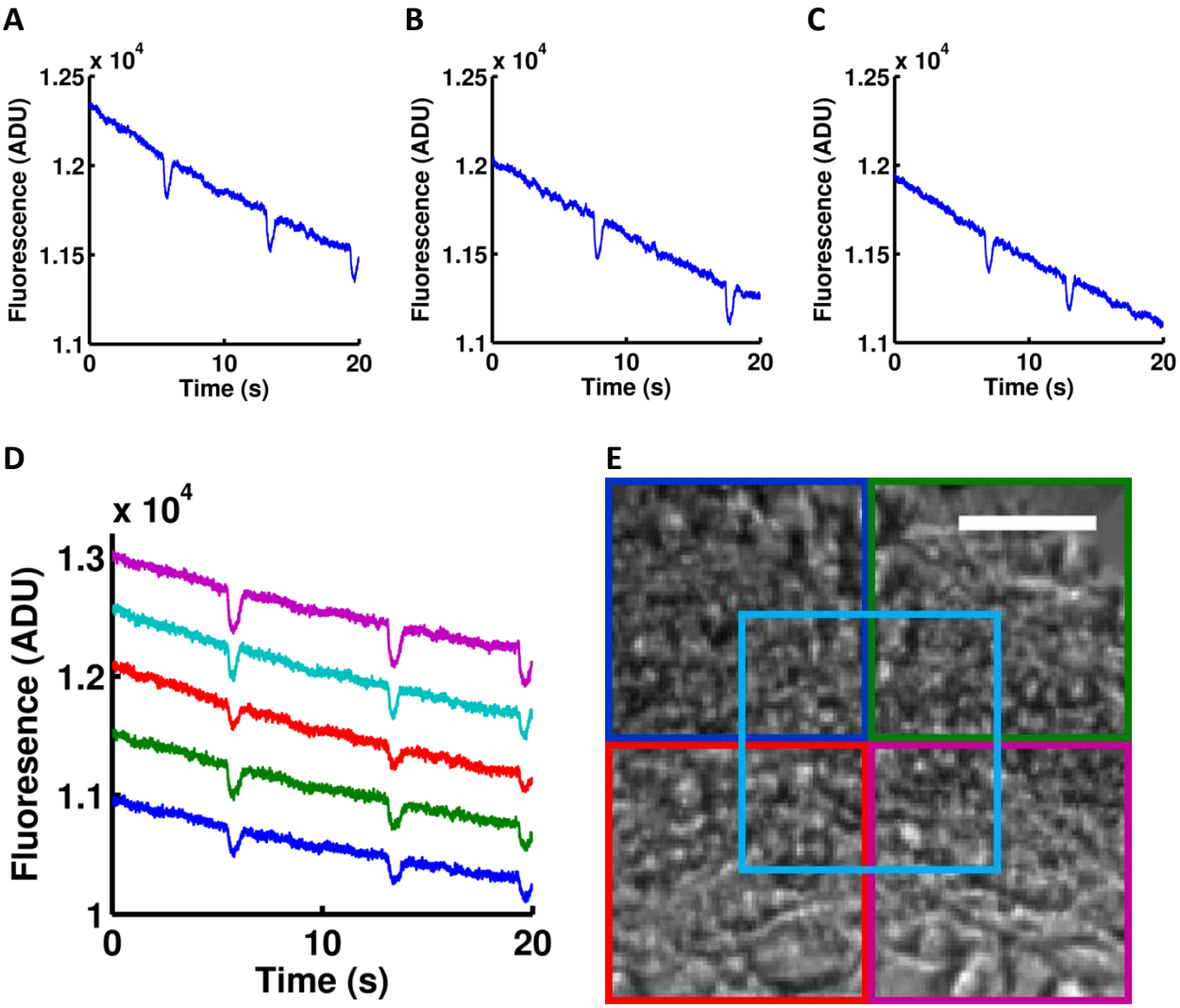

Figure S4: Fluorescence changes in cardiomyocyte syncytia are not due to contractile movement. (*A*, *B*, *C*) Motion in the z-axis that takes the syncytium out of the microscope's focal plane would result in fluorescence signals similar to what we see in (*A*), the unprocessed ICG fluorescence from a cardiomyocyte syncytium (same data as Fig. 3 *B* in the main text). However, intentionally focusing the microscope above (*B*) or below (*C*) the syncytium should produce the opposite effect, as the syncytium would move into the new focal plane, increasing fluorescence during each contraction. Instead, all focal planes display similar behavior, suggesting that no prominent z-axis motions are responsible for observed ICG fluorescence changes. (*D*, *E*) Similarly, motion in the x-y plane could decrease fluorescence by removing bright areas or bringing dim areas into the field of view. In this case, different parts of the field of view should have drastically different signals with some regions displaying net increases in fluorescence by chance. Instead, we observe in (*D*) a systematic decrease in fluorescence in each individual syncytial quadrant; the quadrants are mapped in (*E*): left-upper, blue; right-upper, green; right-lower, magenta; left-lower, red; center; cyan. In all panels, ADU stands for analog-to-digital units, the camera output. The scale bar is 40 μm.

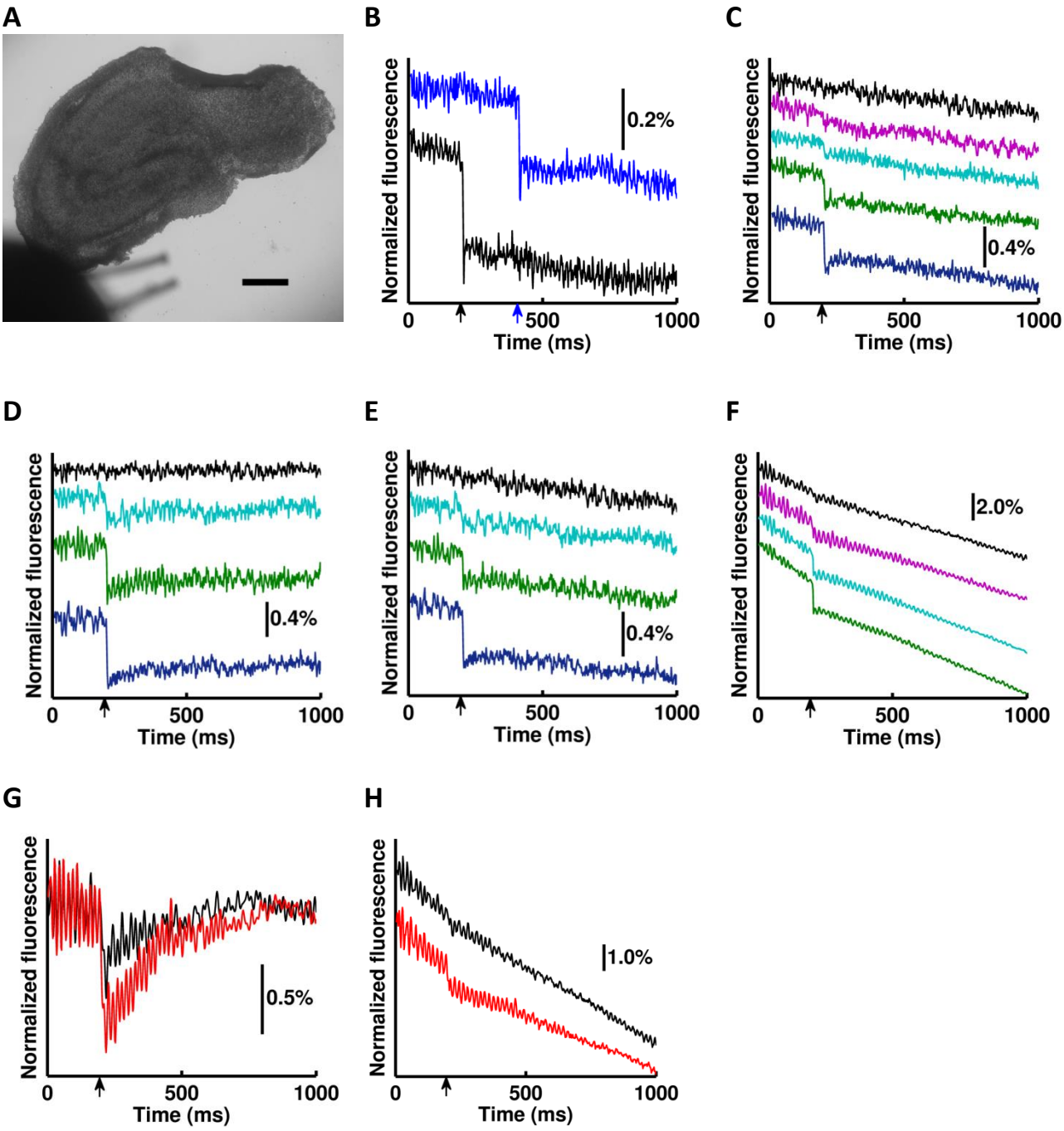

Figure S5: Hippocampal slices show clear ICG fluorescence changes as a result of electrical activity. (*A*) Cultured hippocampal brain slices from neonatal rats maintain glial cells and the three-dimensional structure of the hippocampus. In the lower left of the image, the bipolar stimulating microelectrodes can be seen. The scale bar is 0.5 mm. (*B*) Unprocessed data of slice stimulations at 200 ms (*bottom trace*, *black*) and 400 ms (*top trace*, *blue*) after recording. Changing the timing of the stimulus pulse (*black* and *blue* arrows for the bottom and top traces, respectively) changes the timing of the ICG fluorescence change. For this and subsequent panels, traces are offset vertically for clarity and the scale bar shows the size of a given relative fluorescence change. (*C*) As in Fig. 3 *C*, with stimuli of varying

intensities (*black* – no pulse; *magenta*, *cyan*, *green*, and *blue*, in order of increasing stimulus amplitude), but data is unprocessed. All unprocessed data in this figure is an average of all pixels in the image and has no filtering or bleach correction. (*D*) Similar to *C*, but the duration of the stimulus pulse is varied rather than the intensity (*black* – no pulse; *cyan* – short; *green* – intermediate; *blue* – long). (*E*) As in *D*, but unprocessed data. (*F*) Fig. 3 *D* of gradual tetrodotoxin (TTX) block (*green* – before TTX; *cyan*, *magenta*, *black* – increasing time after TTX), shown here without processing. (*G*) Following washout of TTX, excitability and ICG response were partially recovered (*black* – before washout, same as *black* in Fig. 3 *D*; *red* – 5 minutes after washout). Partial recovery is unsurprising as completely removing TTX block is often impractical (1). (*H*) The data shown in *G* without processing. As the unprocessed traces (*B*, *C*, *E*, *F*, and *H*) demonstrate, potential artifacts that could arise from our data processing are not responsible for the observed changes in ICG fluorescence.

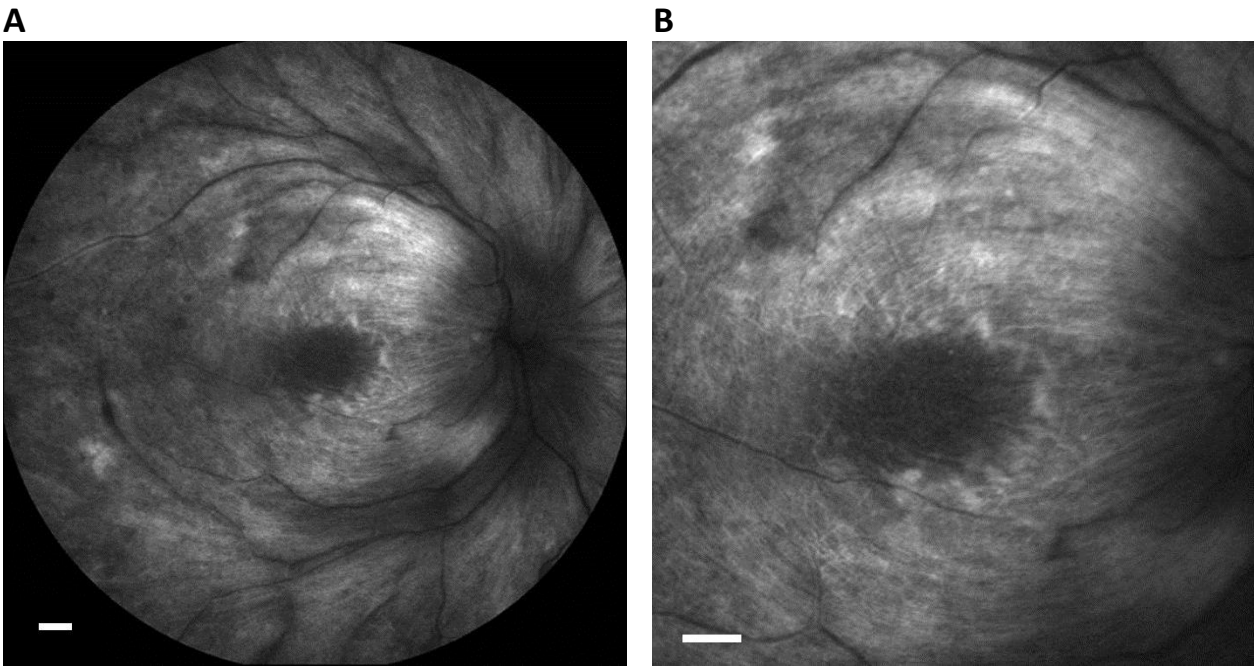

Figure S6: ICG labels retinal ganglion cells (RGCs) in patients after a common ophthalmological procedure. (*A*) ICG intraoperatively applied to the retina of a patient with retinitis pigmentosa clearly stained RGC axons when observed with a scanning laser ophthalmoscope on post-operative day 1. Blood vessels (dark branching structures) converging at the optic disc (dark circular region on far right) show little to no ICG fluorescence due to the rapid rate of ICG clearance from blood. The dark region in the center of the image is the macula with its much lower RGC density. Strong ICG fluorescence (seen in *white)* is clearly seen in numerous RGCs running parallel to each other as they arc from the macula to the optic disc to form the optic nerve, as expected. The scale bar is 800 μm. Observation of ICG voltage dependence in human patients has not yet been attempted. (*B*) A higher magnification image of the same retina, more clearly showing RGC fibers running from the macula (center of image) to the optic disc (right border of image). The scale bar is 800 μm.

Methods

Optical Equipment

ICG fluorescence was monitored using an Evolve 128 EMCCD camera (Photometrics, Tucson, Arizona) attached to an Olympus IX71 inverted microscope (Center Valley, Pennsylvania). The camera CCD is 128x128 pixels and can acquire images at up to 500 Hz full-frame. Binning pixels allowed us to acquire images at 1.8 kHz for preparations in which high spatial resolution was unnecessary, such as oocytes and individual neurons. The dye was excited with a 780 nm diode laser (World Star Technologies, Toronto, Canada), and the Indocyanine Green filter set from Chroma Technology Corp. (49030 ET, Bellows Falls, Vermont) was used to isolate fluorescence emission. Various microscope objectives were used for different preps ranging from a 20X/0.45NA air lens to a 60X/1.45NA oil immersion lens. Raw excitation power varied widely depending on the objective lens in use, but illumination intensity was typically about 0.5 W/cm^2. Retinal imaging was performed using a scanning laser ophthalmoscope (HRA-2, Heidelberg Engineering, Heidelberg, Germany). Excitation of ICG was performed at 795 nm and emission was imaged at wavelengths longer than 810 nm using a 30 degree field of view.

Electrophysiological Equipment

Two-electrode voltage clamp was performed with a Warner Instruments OC-725A amplifier (Hamden, Connecticut). For current clamp, a 100 MΩ resistance was placed in series with the oocyte. Micropipettes were pulled to approximately 0.5 MΩ on a Flaming/Brown micropipette puller (Sutter Instruments, Novata, California, model P-87) and filled with 3 M KCl. Stimulation of rat brain tissue was accomplished via a homemade platinum bipolar field electrode. Patch-clamp of cultured cells was performed using a Dagan 3900 integrating patch clamp amplifier (Minneapolis, Minnesota). Patch pipettes were pulled to approximately 5 MΩ on a CO_2 laser micropipette puller (Sutter Instruments, model P-2000), fire polished immediately prior to use, and filled with patch pipette solution (see Materials and Solutions below). Amplifier outputs were filtered through an 8-pole low-pass Bessel filter (Frequency Devices, Ottawa, Illinois, model 950L8L) and digitized with an SBC-6711-A4D4 data acquisition board (Innovative Integration, Simi Valley, CA). Filter cutoff frequency was set to approximately one fourth of the digitizing sample frequency. The acquisition board was also used to control the clamp and synchronize optical and electrical acquisitions. Software programs for both electrical control and camera control were written in-house.

Tissue preparation protocols

Oocytes were digested in OR2 with collagenase and bovine serum albumin added and incubated in SOS. Excitocytes were prepared by coinjecting cRNAs of Nav1.4 α and β subunits with cRNA of a clone of the Shaker Kv channel with fast inactivation removed as described previously (2) and waiting 2-4 days for channels to express sufficiently. Uninjected oocytes were labeled in 0.0155 mg/ml (20 μM) ICG in SOS for 5-15 minutes. Labeled oocytes were then rinsed and recorded in SOS. Labeling and recording protocols for excitocytes were identical to those for uninjected oocytes apart from the recording solution which had reduced calcium in excitocyte recordings. Oocyte recordings were performed at

room temperature of around 19 °C. Excitocyte recordings were performed at room temperature of around 19 °C, except for tests of high frequency firing, which were performed in a bath at around 30 °C.

Dorsal root ganglia were harvested from spinal cords taken from P2-P6 Sprague-Dawley rats and digested to isolate individual neurons. These cells were then cultured in DMEM (supplemented with 10% fetal bovine serum and 100 U/ml of penicillin and 100 μg/ml of streptomycin) for 24 hours prior to recording. Immediately prior to use, cells were rinsed in patch bath solution, labeled in 0.00775 mg/ml (10 μM) ICG for one to two minutes and rinsed in patch bath solution again for recording. Neuron recordings were performed at room temperature.

Cardiomyocytes were cultured from hearts harvested from P1 neonatal Wistar rats. Hearts were digested in EBSS with 0.08% trypsin similar to prior descriptions (3). Modifications to the protocol included shaking in an incubator rather than on a magnetic stirrer and substituting EBSS with fetal bovine serum for cold culture media with a trypsin inhibitor. Cells were plated on glass coverslips coated in fibronectin. Cardiomyocytes were incubated in DMEM with 10% fetal bovine serum and 100 U/ml of penicillin and 100 μg/ml of streptomycin added. Cardiomyocytes were labeled in 0.00155 mg/ml (2 μM) ICG in DMEM for 1-10 minutes. Cardiomyocyte recordings were performed at 24 °C.

Hippocampal cultured brain slices were prepared as described previously (4, 5). During labeling and prior to recording, slices were kept in a humidified carbogen (95% O_2 / 5% CO_2) atmosphere in a pipette tip box, similar to prior descriptions (6). Slices were labeled in .031 mg/ml (40 μM) ICG in GBSS for 15-20 minutes. Slices were subsequently rinsed in GBSS and recorded in fresh GBSS. Tetrodotoxin stock was diluted to 1 μM in GBSS immediately before use. After application, it was washed out with fresh GBSS. All brain slice solutions were bubbled with carbogen prior to use. Brain slice recordings were performed at room temperature; activity was stimulated with a field electrode using symmetric bipolar pulses to prevent electrode polarization. The maximum stimulus duration was 6 ms in total (a 3 ms pulse in one polarity immediately followed by a 3 ms pulse in the opposite polarity).

All tissue harvesting was performed in accordance with protocols approved by the University of Chicago Animal Care and Use Committee.

For the retinal images, a 0.08 mg/ml ICG in a 5% dextrose solution was directly applied to the retina of a patient with retinitis pigmentosa to aid in peeling the epiretinal membrane during a surgical procedure. The patient's retina was imaged one day after this procedure.

Materials and Solutions

Indocyanine green was obtained in both the clinical formulation as IC-Green (Akorn, Lake Forest, Illinois) and non-clinical formulation as Cardiogreen (Sigma-Aldrich, St. Louis, Missouri). No appreciable differences were found between the two sources. Dye was dissolved in DMSO at a concentration of 20 mM and stored in aliquots at -80 °C. Immediately prior to use, aliquots were thawed and sonicated briefly.

Antibiotics and other salt solution additives: Streptomycin (Sigma-Aldrich), penicillin (Sigma-Aldrich), gentamicin (Sigma-Aldrich), trypsin-TRL3 (Worthington, Lakewood, New Jersey), fetal bovine serum (ATCC, Manassas, Virginia), and DNaseI (Sigma-Aldrich)

Tetrodotoxin (Abcam, Cambridge, United Kingdom) was stored in a 3 mM stock solution in water.

Concentrations are in mM unless otherwise stated

OR2: 82.5 NaCl, 2.5 KCl, 2 $MgCl_2$, 10 HEPES, pH 7.4

Standard oocyte solution (SOS): 96 NaCl, 2 KCl, 1 $MgCl_2$, 1.8 $CaCl_2$, 10 HEPES, pH 7.4, 50 μg/ml of gentamicin

Excitocyte recording solution: Same as SOS but with 0.6 $CaCl_2$ and no gentamicin

EBSS: 132 NaCl, 5.3 KCl, 1 NaH_2PO_4, 10 HEPES, 5.5 glucose, pH 7.4

DMEM: HyClone-DMEM/High Glucose with high glucose, L-glutamine, sodium pyruvate, and phenol red (LifeTechnologies, Carlsbad, California, currently GELifeSciences, Piscataway, New Jersey)

Patch bath solution: 132 NaCl, 6 KCl, 1.8 $CaCl_2$, 1.2 $MgCl_2$, 10 HEPES, 5 glucose, pH 7.4

Patch pipette solution: 150 KF, 10 NaCl, 4.5 $MgCl_2$, 2 ATP, 9 EGTA, 10 HEPES, pH 7.4, filtered

GBSS (Sigma) or made with 137 NaCl, 5 KCl, 1.5 $CaCl_2$, 1 $MgCl_2$, 2.7 $NaHCO_3$, 0.22 KH_2PO_4, 0.28 $MgSO_4$, 0.85 Na_2HPO_4, 5.6 glucose, pH 7.4

Data Analysis

Movies were converted into time-dependent traces by averaging pixel values for each frame of a given movie. Images of oocyte membranes and cardiomyocyte syncytia showed relatively little variation in signal size across different regions of the field of view, so all pixels of each frame were used. Dorsal root ganglion neurons, in contrast, occupied only about 30% of the field of view, so a level threshold was used to isolate neuronal pixels from the non-fluorescent background. Finally, the hippocampal slices contained regions that were largely quiescent. Although the voltage-dependent signal was clearly visible when averaging all pixels, the signal-to-noise ratio was greatly improved by selecting only regions of the image that displayed the most voltage sensitivity. These regions were located by first identifying the single pixels which contained the largest signal and then using morphological image processing to create a binary mask for the image. Morphological operations were based on a diamond-shaped structuring element and utilized repeated openings and closings. Although the exact parameters used were arbitrarily chosen, the resulting signal was qualitatively insensitive to exact choices of morphological parameters. The net effect of these operations was to delineate regions enriched in active pixels and reject the remainder of the image. Once a mask was defined for an image, it was applied to all frames in the movie so that the same pixels would be averaged in each frame to create the time-dependent trace. All traces shown in this work are derived from single acquisitions with no averaging of separate movies.

Once movies had been converted into time-dependent traces by averaging some or all pixels in each frame, the traces were corrected for photobleaching. This was achieved by fitting an exponential curve to all parts of the trace which did not exhibit a voltage-dependent signal and then subtracting this fitted curve from the original trace. In most cases a single exponential function was sufficient to provide a good fit of bleaching. Fluorescence traces from dorsal root ganglion neurons and hippocampal slices were digitally filtered with a low-pass Gaussian filter to reduce high-frequency noise.

Fluorescence traces were normalized by dividing all data points by the average fluorescence at the beginning of each trace before induction of any voltage change. To produce the fluorescence versus voltage graph, $\Delta F/F_o$ was found by taking the average of two regions, one before voltage induction (F_o) and another during voltage induction; the difference between these two averages (ΔF) was then divided by F_o. This value was calculated for each voltage trace and plotted against the membrane potential commanded during voltage induction.

Supporting References

1. Narahashi, T., J.W. Moore, and W.R. Scott. 1964. Tetrodotoxin Blockage of Sodium Conductance Increase in Lobster Giant Axons. J. Gen. Physiol. 47: 965–974.

2. Shapiro, M.G., M.F. Priest, …, F. Bezanilla. 2013. Thermal Mechanisms of Millimeter Wave Stimulation of Excitable Cells. Biophys. J. 104: 2622–2628.

3. Fu, J., J. Gao, …, P. Liu. 2005. An Optimized Protocol for Culture of Cardiomyocyte from Neonatal Rat. Cytotechnology. 49: 109–116.

4. Pusic, A.D., Y.Y. Grinberg, …, R.P. Kraig. 2011. Modeling neural immune signaling of episodic and chronic migraine using spreading depression in vitro. J. Vis. Exp. JoVE. 52.

5. Pusic, A.D., K.M. Pusic, …, R.P. Kraig. 2014. IFNγ-stimulated dendritic cell exosomes as a potential therapeutic for remyelination. J. Neuroimmunol. 266: 12–23.

6. Carlson, G.C., and D.A. Coulter. 2008. In vitro functional imaging in brain slices using fast voltage-sensitive dye imaging combined with whole-cell patch recording. Nat. Protoc. 3: 249–255.